

QUANTUM SIMULATION OF RKKY INTERACTION IN A
TRIANGULAR LATTICE USING THE TRAPPED ION SYSTEM



A thesis submitted towards partial fulfilment of
BS-MS Dual Degree Programme

by

K. SRIRAM

under the guidance of

REJISH NATH

ASSISTANT PROFESSOR

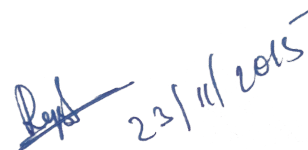
INDIAN INSTITUTE OF SCIENCE EDUCATION AND RESEARCH
PUNE

Certificate

This is to certify that this thesis entitled “Quantum Simulation of RKKY Interaction in a triangular lattice using the trapped ion system” submitted towards the partial fulfilment of the BS-MS dual degree programme at the Indian Institute of Science Education and Research Pune represents original research carried out by K Sriram at Indian Institute of Science Education and Research Pune, under the supervision of Dr Rejish Nath during the academic year 2014-2015.



Student
K SRIRAM



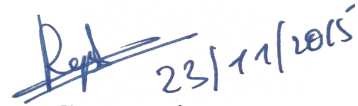
Supervisor
REJISH NATH

Declaration

I hereby declare that the matter embodied in the report entitled “Quantum Simulation of RKKY Interaction in a triangular lattice using the trapped ion system” are the results of the investigations carried out by me at the Department of Physics, Indian Institute of Science Education and Research Pune, under the supervision of Dr Rejish Nath and the same has not been submitted elsewhere for any other degree.



Student
K SRIRAM



Supervisor
REJISH NATH

Acknowledgements

I would like to thank Dr Rejish Nath for guiding me throughout the project and providing assistance academically as well as personally. I would like to thank Dr. G. Venketeswara Pai from HRI who helped me with some concepts relating to Condensed matter Physics and also helped improve this thesis. I would also like to thank Aniruddha Bapat who worked on the initial parts of the project. I would like to thank the IISER Pune computing cluster whose resources have been used in this project. I also appreciate the assistance provided by the IISER Pune Physics department and especially the dean for giving me the chance to complete the project.

On a personal level I would like to thank IISER Pune which had been training me for the past five years and made me the student I am. I would also like to thank my parents who have always supported me in all my endeavours.

Abstract

Using trapped ion quantum simulation system we create RKKY-like interaction pattern in a crystal having quantum spins in a triangular lattice. Thereafter we study its properties and see whether it can be used to simulate any system especially spin glass.

Contents

| | | |
|----------|---|-----------|
| 1 | Introduction | 1 |
| 1.0.1 | RKKY Interactions | 2 |
| 2 | Quantum Simulation of Ising spin models in trapped ion crystals | 4 |
| 2.1 | Equilibrium configuration of trapped ions | 4 |
| 2.2 | Computational aspects of determining the equilibrium configuration | 6 |
| 2.2.1 | Initial Configuration used for solving | 6 |
| 2.2.2 | Stability of a configuration | 7 |
| 2.3 | Vibrational Spectrum of an Ion Crystal | 8 |
| 2.4 | Quantum Simulation using ion crystals | 10 |
| 2.4.1 | Computational resources used | 15 |
| 2.4.2 | Generating power law spin-spin interactions | 16 |
| 2.4.3 | Beyond power law potentials | 16 |
| 2.5 | Summary | 19 |
| 3 | Quantum Simulation of RKKY Interactions in a triangular lattice using trapped ions | 20 |
| 3.1 | Simulating RKKY Interactions | 20 |
| 3.2 | Spin Glass with trapped ions | 25 |
| 4 | Conclusion | 26 |
| | References | 27 |
| A | Long proofs | 34 |
| A.1 | Determining the equilibrium configuration of two dimensional crystals | 34 |
| A.2 | Derivation of the spin-spin Hamiltonian | 36 |

Chapter 1

Introduction

There are many quantum systems that are difficult to study analytically. To study a quantum system numerically using classical computers requires an exponential increase in computing power for a linear increase in the size of the system. The only way one can study such systems is by using quantum simulations [1] i.e. by using controllable quantum mechanical systems. Quantum many body systems particularly benefit from such an approach. Deutsch[2] had shown that there even exist mathematical problems which are better solved by quantum systems than classical ones and Shor[3] had discovered the Shor's Algorithm, a method to factorize numbers using quantum systems which is exponentially faster than any classical algorithm.

Cirac and Zoller[4], using trapped ion, had for the first time shown that a quantum computer can be implemented. The major part was to show a controlled bit-flip operation. Weinberg's group[5] had experimentally demonstrated how to do it. This led to proposals and realisations of various protocols of quantum computation. Gulde et al.[6] implemented the Deutsch-Josza algorithm in a single ion. Barret et al. and Riebe et al.[7, 8] demonstrated the teleportation of a single qubit in a two-ion trap. Chiaverini et al.[9] were able to implement a quantum error correction protocol (as suggested by Shor) using trapped ions. Error correction is critical to make the system scalable.

Using the trapped ion technology many quantum simulations have been realised in the past decades, such as the topological hexagonal Kitaev model [10], fermionic lattices [11], SU(2) Ising models [12, 13, 14, 15, 16] -including frustrated magnetism [17, 18, 19] and, very recently, to the observation of entanglement dynamics in spin chains [20, 21] and topological quantum spin liquids[22]. Besides these studies, which are implemented in linear-(1D) ion crystals, quantum simulation of various spin models has also been proposed in 2D ion-crystals [23, 24, 25].

Development of and challenges in Quantum Computation using the trapped ions system have been discussed in reviews [26, 27, 28, 29, 30, 31]. More specifically a review of quantum simulation of many body systems with trapped ions is given in [32].

1.0.1 RKKY Interactions

The following interactions are mediated via an indirect exchange coupling of the respective spins and the spin of conduction electrons:

1. The interaction between magnetic dipoles of the magnetic ions in dilute alloys of magnetic ions in a non-magnetic metals such as Mn in Ag.
2. The interaction between nuclear spins in molecules or metals. This has been observed using Nuclear Magnetic Resonance experiments.
3. The interaction between the spins of 4f electrons in rare-earth metals.

The magnetization of the conduction electron gas in the vicinity of magnetic ions shows an oscillatory behaviour[33]. This causes the indirect coupling between the spins, with the magnetization of the conduction electron gas as exchange medium. This is the RKKY interaction pattern, first proposed by Ruderman and Kittel [34] in the context of nuclear spins and later extended and generalised by Kasuya [35] and [36] using their work on alloys of magnetic ion cores in non-magnetic metals. For magnetic spins \vec{I}_i and \vec{I}_j , located at \vec{r}_i and \vec{r}_j , in such an above system, they showed that the interaction Hamiltonian $\hat{\mathcal{H}}_{ij}$ between the spins is of the form:

$$\hat{\mathcal{H}}_{ij} = \frac{\vec{I}_i \cdot \vec{I}_j}{4} \frac{|\Delta k_m k_m|^2 m^*}{(2\pi)^3 r_{ij}^4 \hbar^2} (2k_m r_{ij} \cos(2k_m r_{ij}) - \sin(2k_m r_{ij})) \quad (1.1)$$

where, $|\Delta k_m k_m|$ represents the strength of the interaction between the magnetic ions and conduction electrons, m^* is the effective mass of the conduction electrons, r_{ij} the distance between the spins, and k_m is the wavenumber of the Fermi surface of the host metal. Over relatively large distances (not in the immediate vicinity) this can be approximated to:

$$\hat{\mathcal{H}}_{ij} = \frac{\vec{I}_i \cdot \vec{I}_j}{4} \frac{2k_m |\Delta k_m k_m|^2 m^*}{(2\pi)^3 r_{ij}^3 \hbar^2} \cos(2k_m r_{ij}) \quad (1.2)$$

Note that the interaction oscillates between ferro-magnetic and anti-ferromagnetic nature. This indirect coupling plays crucial roles in Kondo effect and in Spin

Glasses. In Kondo Effect[37, Ch. 8] a minimum is observed in resistivity versus temperature of dilute magnetic alloys of non-magnetic metals, this is due to the very large scattering probabilities of conduction electrons at the magnetic centres in low temperatures.

In noble metals weakly diluted with magnetic metal ions, below a certain temperature, a new kind of order called spin glass is observed[38]. All magnetic moments appear to have frozen in random directions with no long range order whatsoever.

One of the phenomenon found is a special kind of spin ordering known as spin glass phase [38]. It arises in noble metals with magnetic impurities below a certain temperature. The interaction between any two spins in this system is the RKKY interaction, which is oscillatory. Since the distances between magnetic metal ions will be more or less random, the nature (whether ferromagnetic or antiferromagnetic) of the interaction between two spins is also random. In such a case no configuration can be found which will satisfy all the couplings. This is marked by several unusual characteristic such as a highly disordered ground state configuration, freezing of the magnetic moments over long periods of time, a characteristic peak in the non-linear susceptibility versus temperature graph at the critical temperature where such behaviour is seen. Edwards and Anderson developed a model[39] to describe the behaviour of this system. Later such behaviour has been observed in more systems and various theoretical models. Spin glass research has provided mathematical tools to analyse some interesting real-world problems in fields such as statistical physics, condensed matter physics, graph theory and complexity theory [40]. Even today the field still has many open questions.

We propose to engineer a method to simulate RKKY interactions between ions in a triangular lattice of trapped ions. We shall demonstrate how this can be achieved. We shall also explore possible ways in which these RKKY interactions can be used to simulate Spin Glass.

Chapter 2

Quantum Simulation of Ising spin models in trapped ion crystals

In this chapter we shall review how to simulate an effective Ising Hamiltonian using trapped ions. We start with a section describing how ions are trapped. We shall calculate the shape and size of the crystals that are formed. Then we shall calculate the structure of the phonons that are present in the system. Our scheme of creating a quantum simulation uses phonons as the exchange medium between qubits. We shall then show how to perform the quantum simulation and derive an effective Ising Hamiltonian. We shall conclude the chapter with an example of the implementation.

2.1 Equilibrium configuration of trapped ions

Usually Alkali-earth metal ions such as Ca^+ , Sr^+ or Ba^+ are used as they have Hydrogen-like electronic structure, hence the electronic states are easier to study and use. For the purposes of these simulations usually 2D Paul traps [41, 42, 43, 44] or Penning traps [45, 46] are used. Recent work in a Penning trap has demonstrated controllable spin-spin interactions between a few hundred ionic spins [16], whereas studies in Paul traps show excellent prospects for implementing such interactions as well. The net effect of a trap on the ions although might be complicated can be approximated by a pseudopotential similar to a harmonic oscillator, where the potential rises quadratically. The strength of these traps can be represented using trapping frequencies which is analogous to the angular frequency of a harmonic potential. The trapping frequency is usually in the range 1 MHz to 50 MHz. This results in inter-ion distances of about 0.1 μm to 10 μm . The ions crystallize into self organized coulomb crystals. We shall calculate the positions of the

ions in such crystals. This is an adaptation into three dimensions of a calculation done for one dimensional chains by James[50]. We shall assume that the pseudo-potential experienced by N ions due to the traps is of the form:

$$V = \frac{1}{2}M\nu_0^2 \sum_{i,d=1,1}^{N,3} \nu_d^2 x_{d,i}^2 \quad (2.1)$$

Here, d represents the direction such that x_1, x_2 and x_3 represents the x, y and z coordinates respectively. $\nu_0\nu_d$ is the trapping frequency along the direction d where ν_0 represents the scale of the frequency and ν_d represent the ratios in the respective directions. This tells us how strong the confinement is along a particular direction, M is the mass of the ions and \vec{x} represents their position. All the ions are in a single trap. They face coulombic repulsions from each other and hence the total potential experienced by all the ions will be:

$$V = \frac{1}{2}M\nu_0^2 \sum_{i,d=1,1}^{N,3} \nu_d^2 x_{d,i}^2 + \sum_{\substack{i,j=1,1 \\ i \neq j}}^{N,N} \frac{Z^2 e^2}{8\pi\epsilon_0 r_{ij}} \quad (2.2)$$

Here Z is the degree of ionization of the ions, e is the electron charge, ϵ_0 is the permittivity of free space and r_{ij} is the distance between two ions.

To simplify our calculations we shall write the positions in terms of a characteristic length defined by:

$$u_d = x_d/l$$

where,

$$l^3 = \frac{Z^2 e^2}{4\pi\epsilon_0 M\nu_0^2}$$

This length is of the order of the distances between the ions, for most experiments this is in the range $0.1\mu\text{m}$ to $10\mu\text{m}$. This lets us rewrite the potential energy as:

$$V = \frac{1}{2}M\nu_0^2 l^2 \left(\sum_{i,d=1,1}^{N,3} \nu_d^2 u_{d,i}^2 + \sum_{\substack{i,j=1,1 \\ i \neq j}}^{N,N} \frac{1}{u_{ij}} \right) \quad (2.3)$$

We shall calculate the equilibrium configuration of the ions in this potential assuming the ions to be classical objects. This is done by finding a minimum of the potential energy function by numerically calculating zeros of the gradient of the potential energy function by using a multidimensional

non-linear Newton's method[51]. The gradient of (2.3) is (refer to appendix A.1 for the derivation):

$$\frac{\partial V}{\partial x_{d_i,i}} = M\nu_0^2 l \left(\nu_{d_i}^2 u_{d_i,i} + \sum_{\substack{j=1 \\ i \neq j}}^N \frac{u_{d_i,j} - u_{d_i,i}}{u_{ij}^3} \right) = 0 \quad (2.4)$$

2.2 Computational aspects of determining the equilibrium configuration

In this section we look into the following problems that were encountered while calculating the equilibrium configuration of ions: 1. Determining appropriate initial conditions of positions to used for the numerical calculations. 2. Determining if a particular configuration is stable. 3. In case multiple stable configurations exist, which one would be more stable. The parameters that are in our control are the trap frequencies and the number of ions. So we need to solve these problems for a wide range of these parameters.

2.2.1 Initial Configuration used for solving

Since we are numerically solving for the positions using Newton's method, we need to provide an initial configuration of ions. If our initial configuration is closer to the actual solution the calculation is more likely to converge and also take less time. In section 2.2.2 we shall see how to decide what will be the general form (whether it will be a linear chain or a two dimensional crystal or something else). Here we shall specify, given a certain form, the appropriate initial configuration to obtain a solution of that form. These have been derived using a process of trial and error, which might have a lack of completeness in its search for all possible configurations. However it is enough if the initial configuration is able to give a solution of the desired form, since then the only remaining problem will be long convergence times which can be solved by fine-tuning these configurations. To know what are the possible forms of the equilibrium configurations a large number of solutions obtained from randomly generated configurations was studied. The solutions obtained can be broadly categorized into the four categories. Here is a brief description of these categories and the initial conditions used:

1. Linear Chain: This is favoured when the trap potentials are strong along two directions and weak along one. The initial configurations for this is easy to arrive at. We used evenly spaced ions in a row along the

direction in which the final solution is expected to be. Along the other two directions the ions are at the minimum of the potential.

2. Planar crystal: These can be subdivided into two more categories for the purposes of determining the initial configuration.
 - (a) Zigzag Chain: This is favoured when trap potentials are strong along one direction, slightly weak along another and very weak along the third. Along the direction with the weakest potential this is similar to the linear chain. Along the next direction the ions are alternating at a certain distance from the potential minimum.
 - (b) Planar isotropic crystal: This is favoured when the trap potentials are almost equal along two directions and stronger along a third. It was found that the most stable planar crystals take the form of concentric rings of polygons. But the question of how many ions should be in each ring still remains. This was selected by looking at the configuration which after solving gave the least value of the potential energy. Table 2.2 tells us the number of ions that should be present in each ring for a given number of total number of ions. It is observed that the ions tend to form a triangular lattice. This realized if the total number of ions is 7,19,38
3. Three-dimensional Crystal: This is favoured when the trap potentials are almost or completely equal. There seem to be no simple general rules which can be followed to obtain a good initial configuration and one has to do a case by case study depending on the total number of ions.

Figure 2.1 shows the above mentioned forms of ion crystals.

2.2.2 Stability of a configuration

As discussed in section 2.1, we calculate the equilibrium configuration of ions by numerically solving for the derivative of the potential. This will only give us a fixed point of the potential which may or may not be a stable. If the system were stable, given any small perturbation the system should return to its original state. A small perturbation to the system can be represented as a combination of the vibrational modes (as will be discussed in 2.3. According to the theory of small oscillations, if a vibrational mode is stable it will have a positive frequency. So the stability of a particular configuration can be determined by looking at the presence or absence of a vibrational mode with a negative frequency. In figure 2.2 we plot the frequency of the lowest

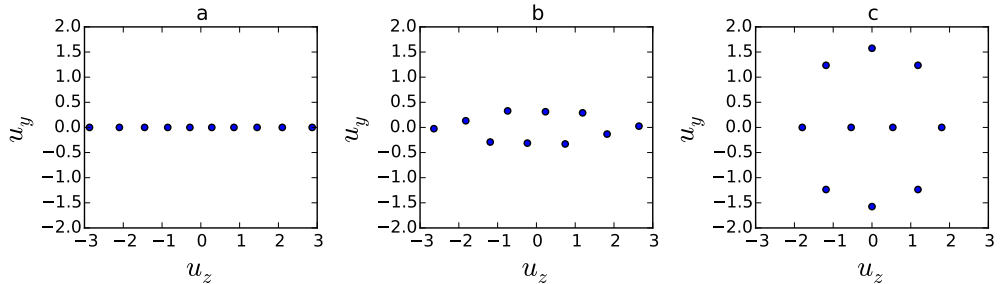


Figure 2.1: This figure depicts the various crystal phases for 10 ions. The diagrams show the position of ions on the z-y plane for (a) liner chain (b) zigzag chain (c) 2d crystal.

frequency transverse mode as a function of the transverse trapping frequency for the linear chain and a planar crystal.

From the figure 2.2, we can conclude that at $\nu_y \approx 4.6$ the crystal undergoes a phase transition. Note however that, near this point, the solution obtained using a zigzag chain will look very similar to a linear chain. Using such analysis one can also determine the point where the 2d to 3d phase transition takes place. For the case of $N = 10$ ions we do such a study, using the results we can predict the phase of the structure based on the results for a given set of trapping frequencies as shown in 2.3. We expect similar plots for other number of ions as well.

2.3 Vibrational Spectrum of an Ion Crystal

We shall assume that these ions are situated in the equilibrium positions and the only form of motion are small oscillations about these points. Since the ions interact with each other through Coulomb repulsions their motions will be coupled. We would have to describe these oscillations using independent modes of oscillation, which can be calculated using the theory of small oscillations. To describe the energy in this system, we shall assume the normal modes to be quantum harmonic oscillators. An excitation in one of these modes may be termed a phonon. Since phonons are the exchange media in our quantum simulation, it is essential to calculate the eigenfunctions and eigenfrequencies of all the phonon modes.

According to the theory of small oscillations we need to diagonalize the second derivative of the potential energy function. The second derivative is (derived in appendix A.1):

| N | Configuration | N | Configuration |
|----|---------------|----|---------------|
| 3 | 3 | 12 | 4 8 |
| 4 | 4 | 13 | 4 9 |
| 5 | 5 | 14 | 4 10 |
| 6 | 1 5 | 15 | 5 10 |
| 7 | 1 6 | 16 | 1 5 10 |
| 8 | 1 7 | 17 | 1 6 10 |
| 9 | 2 7 | 18 | 1 6 11 |
| 10 | 3 7 | 19 | 1 6 12 |
| 11 | 3 8 | 20 | 1 7 12 |

Table 2.2: Configuration of ions in two-dimensional crystals. This table tells the number of ions present in each shell of a two dimensional crystal for a given number of ions. This first number is the number of ions in the innermost shell, then the second shell and so on. Note that if the number of ions is 7,19,37... a triangular lattice is formed.

$$\frac{1}{2} \frac{\partial^2 V}{\partial x_{d_i,i} \partial x_{d_j,j}} = \frac{1}{2} M \nu_0^2 \begin{cases} \nu_{d_i}^2 + \sum_{\substack{k=1 \\ k \neq i}}^N \frac{3(u_{d_i,i} - u_{d_i,k})^2 - u_{ik}^2}{u_{ik}^5} & : \begin{matrix} i=j \\ d_i=d_j \end{matrix} \\ - \frac{3(u_{d_i,i} - u_{d_i,j})^2 - u_{ij}^2}{u_{ij}^5} & : \begin{matrix} i \neq j \\ d_i=d_j \end{matrix} \\ - \frac{3(u_{d_i,i} - u_{d_i,j})(u_{d_j,i} - u_{d_j,j})}{u_{ij}^5} & : \begin{matrix} i \neq j \\ d_i \neq d_j \end{matrix} \\ \sum_{\substack{k=1 \\ k \neq i}}^N \frac{3(u_{d_i,i} - u_{d_i,k})(u_{d_j,i} - u_{d_j,k})}{u_{ik}^5} & : \begin{matrix} i=j \\ d_i \neq d_j \end{matrix} \end{cases} \quad (2.5)$$

We shall call the eigenvalues ω_m and the eigenvectors $\vec{\mathbf{b}}_{mi}$. For a system having N ions, there will be $3N$ eigenvalues/eigenvectors.

When we calculate the phonon modes, we observe that the spectrum of frequencies can be distinguished into two bands: one having transverse modes (motion perpendicular to the plane of the ions) and another with longitudinal modes (motion along the plane of the ions). In all cases the band containing the transverse phonons has higher frequencies. We shall be using a laser field which is perpendicular to the plane of the ions and hence can only affect the motion in the transverse direction. Therefore only transverse phonons can affect interactions.

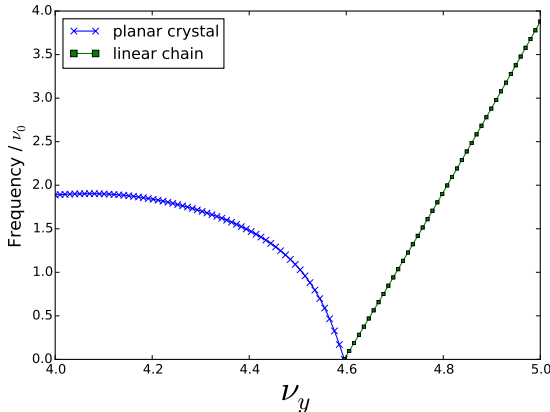


Figure 2.2: This figure plots the frequency of the lowest frequency transverse phonon mode for the linear chain and a specific mode of the planar crystal as a function of the transverse trapping frequency. We can clearly see that about $\nu_y \approx 4.6$ the least frequency phonon mode for both the crystals becomes zero. This indicates a phase transition which occurs at this point. This plot has been made for 10 ions and using $nu_z = 1, \nu_x = 10$.

Phonon modes at the end of a band are easier to use as one can work with larger detunings. Also noise due to other bands are reduced. Developments in techniques of ion-pinning can help us in manipulating the phonon modes as well as their frequencies. One has to look through the phonon modes or engineer them in the desired way as to create the required interaction pattern.

2.4 Quantum Simulation using ion crystals

To perform any form of quantum simulation or quantum computation, we require a method to store our qubits. It should be feasible to manipulate and measure them individually and they should have a large coherence time. In the trapped ion system, superpositions of two electronic states of the ions are used for this purpose. States can be easily initialized using optical pumping techniques and measured by attempting to excite one of the states used to represent the qubit. Two schemes are largely used:

Optical qubits: Here the ground state and an excited metastable state are used to represent the $|0\rangle$ and $|1\rangle$ of our qubits. They are manipulated by lasers in optical frequencies. They have lifetimes of about a second. They require lasers with very high spectral coherence, but allow for easy focussing

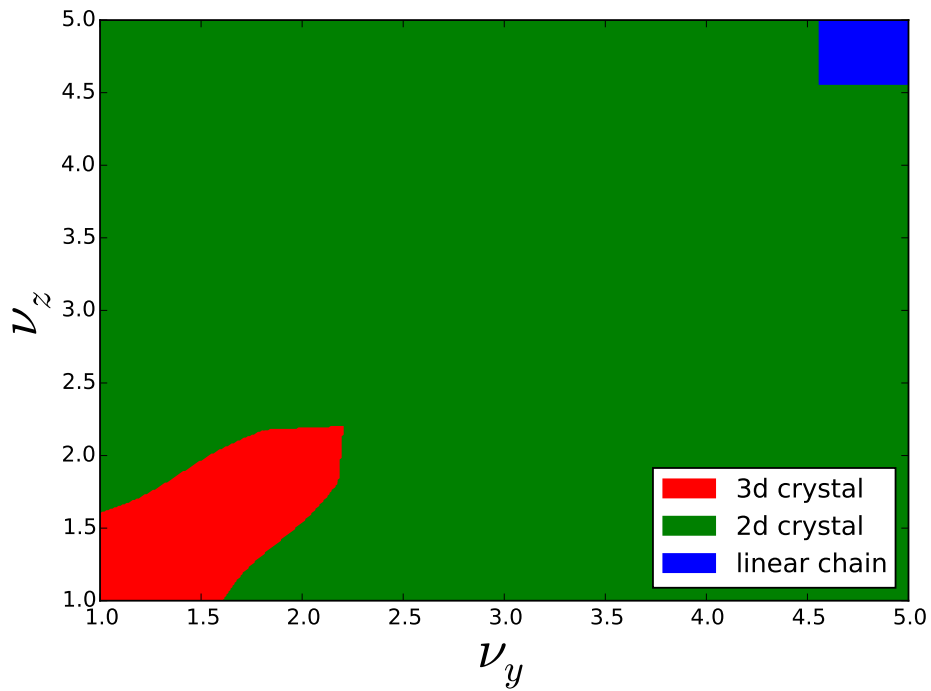


Figure 2.3: This is a phase diagram that shows what would be the form of the crystal for various values of ratios of the trapping frequencies for a system containing 10 ions. ν_x, ν_y and ν_z are trapping frequency ratios. $n\nu_z$ has been taken as 1. The crystal can exhibit a linear phase, a planar crystal phase and a 3d-crystal phase. This figure has been generated numerically by calculating the stability of particular phase by analysing its eigenspectrum of phonon modes. This diagram will help us in determining the values for trapping frequencies to use to generate a particular form of crystal.

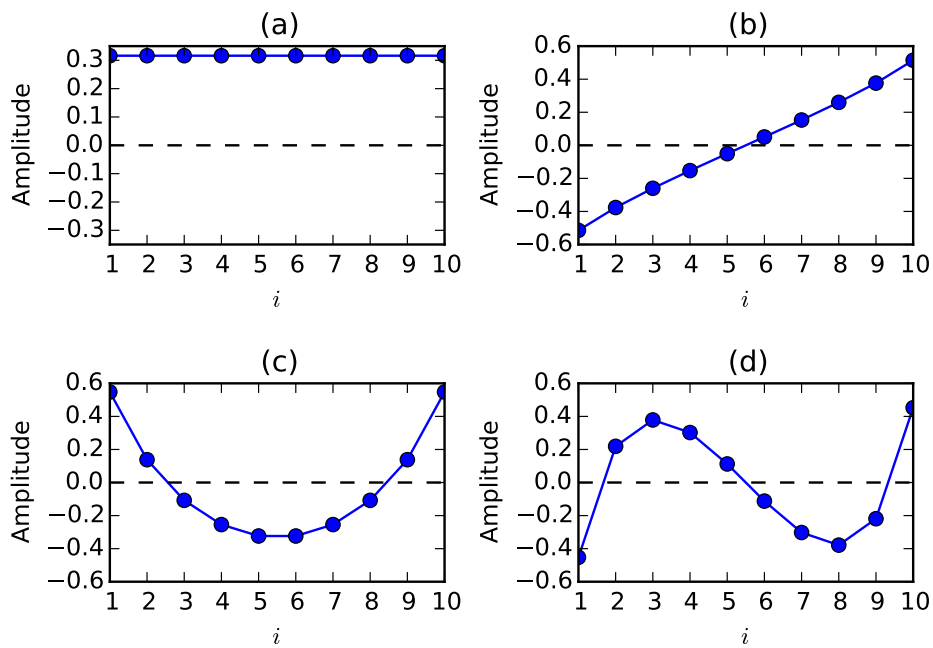


Figure 2.4: These plots show the highest-frequency transverse modes (in decreasing order of frequency) of 10 ions in a linear chain. The x-axis represents the index of each ion. The y-axis represents the relative amplitude of each ion after normalization. The highest mode (shown in (a)) is the centre-of-mass mode in which all the ions oscillate in-phase with the same amplitude.

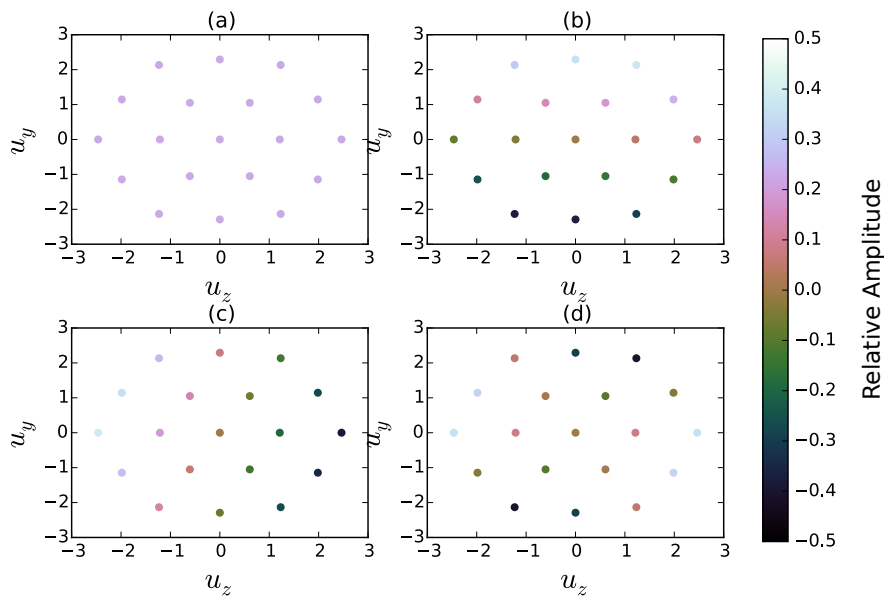


Figure 2.5: These plots show the highest-frequency transverse modes (in decreasing order of frequency) of 19 ions in a two dimensional crystal. The dots represent the ions and the colour of the crystals represents the amplitude.

and operations are of very high fidelity.

Radio-frequency qubits: Here two hyperfine levels of the ground state are used to represent quantum information. These are generally well suited for quantum simulations as the lifetimes of the states are much larger. They can either be directly be manipulated by microwaves or using a Raman process. A Raman process requires two laser fields, an atom absorbs a photon from one of the laser fields and emits into another, the net effect is as though the atom is affected by a laser with a frequency equal to the difference in frequencies of the two laser fields.

The hamiltonian of the system described so far can be represented as a sum of the energy in the electronic state and the energy in the phonons. The electronic state energy would be.

$$\hat{H}_e = (\hbar\omega) \sum_{i=1}^N \hat{\sigma}_i^z \quad (2.6)$$

The motional energy can be represented as a summation of harmonic oscillator Hamiltonians, one for each phonon mode.

$$\hat{H}_m = \sum_{m=1}^{3*N} \hbar\omega_m (\hat{a}_m^\dagger \hat{a}_m + 1/2) \quad (2.7)$$

Here ω_m are the eigenvalues of the phonon modes. \hat{a}_m^\dagger and \hat{a}_m are the annihilation and creation operators of a phonon in mode m .

We propose to indirectly couple the electronic states of each ion using the phonons as the interaction medium. This can be achieved by coupling the electronic states with the motional states. A laser field (or an equivalent Raman process) is used for this purpose. A general Hamiltonian describing the interaction between an optical field and an atom/ion will be:

$$\hat{H}_I = \sum_{i=1}^N \hbar\Omega \left(e^{i(\vec{k}\cdot\vec{x}_i + \omega_I t + \phi_i)} + \text{h.c.} \right) \hat{\kappa}_i \quad (2.8)$$

Here, Ω is the Rabi frequency, indicative of the interaction strength (it depends on the amplitude of the optical field and the transition dipole moment), \vec{k} and ω_I is the wavevector and angular frequency of the applied field respectively (if a Raman process is used this is the difference in the angular frequencies of the two fields used). The angular frequency ω_I used is $\omega_{m'} + \delta$, where m' represents the mode that we propose to use for our interaction. x_i is the position of the ion at site i . Notice that we have assumed that all the ions are uniformly radiated, otherwise all the ions will have their own Ω_i and \vec{k}_i . $\hat{\kappa}_i$ acts on the Bloch space of the states created by the $|0\rangle_i$ and $|1\rangle_i$, it

depends on the polarization of the optical field and the angular momenta of the states encoding $|0\rangle_i$ and $|1\rangle_i$. A general form for $\hat{\kappa}_i$ would be

$$\hat{\kappa}_i = \alpha_0 \hat{\mathbb{1}} + \alpha_1 \hat{\sigma}_i^x + \alpha_2 \hat{\sigma}_i^y + \alpha_3 \hat{\sigma}_i^z \quad (2.9)$$

The total Hamiltonian will be $\hat{H} = \hat{H}_e + \hat{H}_m + \hat{H}_I$. This can be simplified and transformed to be of the form of an Ising Hamiltonian.

$$\hat{H} = \sum_{i=1}^N E_i \hat{\sigma}_{z,i} + \sum_{\substack{i,j=1,1 \\ i \neq j}}^{N,N} J_{ij} \hat{\sigma}_{z,i} \hat{\sigma}_{z,j} \quad (2.10)$$

where J_{ij} takes the following value:

$$J_{ij} = \sum_{m=1}^{3N} \frac{\Omega^2 \eta_i^m \eta_j^m}{\delta_m} \quad (2.11)$$

where δ_m is the detuning of the applied laser field from the phonon mode m . This would be simply $\omega_I - \omega_m$.

$$\eta_{mi} = \vec{\mathbf{k}} \cdot \vec{\mathbf{b}}_{mi} \sqrt{\frac{\hbar}{2M\omega_m}} \quad (2.12)$$

η_{mi} are the Lamb-Dicke parameters. They indicate the strength of the coupling between the electronic states and the motional states. Refer to appendix A.2 for the transformations required to obtain equation (2.10). The derivation assumes the system to be in the Lamb-Dicke regime i.e. the coupling created between the electronic states and the motional states is weak ($\eta_{mi} \sqrt{\langle (\hat{a}_m + \hat{a}_m^\dagger)^2 \rangle} \ll 1$). The rotating wave approximation has also been used in this derivation. From equations (2.11) and (2.12) we can conclude that the interaction pattern would resemble the phonon mode with the smallest detuning.

2.4.1 Computational resources used

The code required for the calculations have been written in Python with the help of the scipy library [52]. LAPACK [53] and ARPACK [54] from FORTRAN have been used to calculate the eigenvalues/eigenvectors. Plots have been made using the matplotlib library [55].

2.4.2 Generating power law spin-spin interactions

Power law interactions are of the form $J_{ij} = r_{ij}^{-\alpha}$; here r_{ij} is the distance between the ions, in the case of a linear chain one can take this to be simply $i - j$, where i and j are the indices of the spins. We can attain values of α such that $0 < \alpha < 3$ by varying the detuning δ . A similar result has been obtained in [16]. There are many interesting models for spin chains under power law potentials viz. Haldane-Shastry Model, Majumdar-Ghosh Model, Meshkin-Lepkov-Glick model [56], which can be studied using such a simulation. However these models assume periodic boundary conditions which will be hard to implement using a linear chain trapped ion system.

We shall show a calculation with 10 ions. First of all we need to prepare a linear chain. Note that this is extendable to more number of ions. A one dimensional Paul trap is a good means to achieve this. Appendix 2.2 can help us with determining the ratio of trapping frequencies to be used. We shall use the parameter values of $\nu_0 = 1$ MHz, $\nu_x = 1$, $\nu_y = \nu_z = 10$. Using equation (2.4) we can calculate the positions of these ions. For our choice of number of ions and trapping frequencies the following would be the positions of ions on a linear line (the ions have been assumed to be of calcium):

| Positions (in 10^{-5} m) | | | | | | | | | |
|----------------------------|-------|-------|-------|-------|------|------|------|------|------|
| -4.88 | -3.57 | -2.47 | -1.45 | -0.48 | 0.48 | 1.45 | 2.47 | 3.57 | 4.88 |

We shall use the data of these positions to solve for the phonon modes in the system. This is done by calculating the eigenvalues and eigenvectors of (2.5). The spectrum of frequencies has been plotted in 2.6 and some of the highest energy transverse modes have been shown in 2.4.

The highest frequency mode has all the ions oscillating in phase with the same amplitude. This is the centre of mass mode. If our detuning from the frequency of this mode is very small, the interaction pattern would resemble the phonon mode. Since the mode has all the ions moving in phase with the same amplitude, the corresponding interaction pattern would be a long range ferromagnetic interaction or $J \sim r^0$. As we increase the detuning, other phonon modes also start playing a role in determining the interaction pattern. We observe that it takes a $J \sim r^{-\alpha}$ form.

2.4.3 Beyond power law potentials

New techniques have led to the development of more complicated spin models recently. Nath et al.[22] have used ion pinning to simulate the Hexagonal Kitaev Model which has a topological spin liquid ground state. Ion pinning

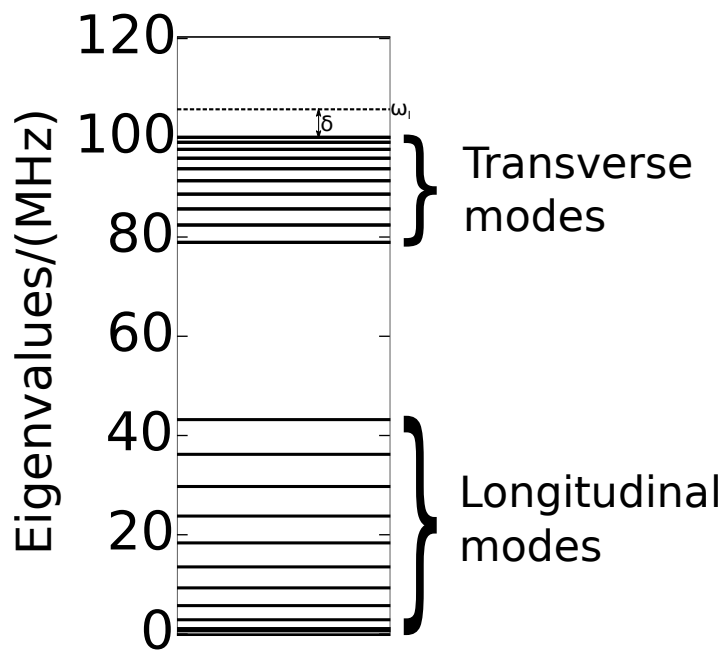


Figure 2.6: The spectrum of phonon modes. We can see that it is divided into two bands. Further analysis shows that the lower band has longitudinal modes (in which the ions vibrate along the chain) and the higher band has transverse modes (in which the ions vibrate perpendicular to the chain). It is the transverse modes that play role in determining the interaction pattern.

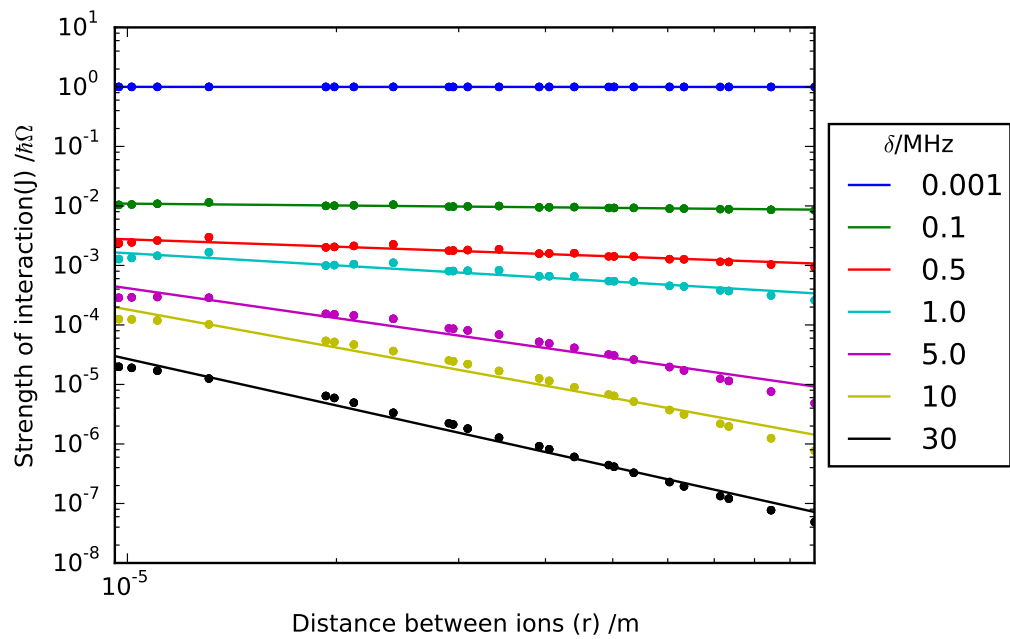


Figure 2.7: A log-log plot of the calculated interaction strength between two ions and the distance between them. Various plots are for different values of detuning. Since the points fall on a straight line in the plot, we can conclude that it follows a power law.

creates different trap frequencies around specific ions, which lets us engineer the phonon modes. Bermudez et al. [25] create frustrated spin models using anisotropic couplings. This is done by using laser fields whose resultant wavevector is not perpendicular to the plane of the crystal. We shall incorporate these techniques to simulate RKKY interactions.

2.5 Summary

In this chapter we have discussed how to use a Paul/Penning trap to trap ions into one and two-dimensional crystals. We simulate Ising spin models using these Ion crystals, specifically power law potentials. We shall use these techniques to develop a simulation of RKKY interactions.

Chapter 3

Quantum Simulation of RKKY Interactions in a triangular lattice using trapped ions

3.1 Simulating RKKY Interactions

In section 2.4.2 we saw how to simulate power law potentials in a one-dimensional linear chain using trapped ions. Now we shall demonstrate how to simulate RKKY Interactions using similar techniques. As discussed in section 1.0.1, RKKY interactions show both ferromagnetic and antiferromagnetic interactions in an oscillatory manner in space. In section 2.4.2 we had utilized primarily the centre of mass phonon mode. This led to an interaction pattern in which all interactions were antiferromagnetic as all ions oscillate in the same phase in the centre of mass mode. Hence to create an oscillatory interaction pattern one could use a phonon mode in which neighbouring ions oscillate out of phase. An analysis of the phonon modes of the linear chain as well as the two-dimensional crystals shows that the lowest frequency transverse modes happen to be of this nature, as can be seen from figure 3.1.

One could utilize this mode to generate RKKY interactions by tuning the effective laser frequency (ω_I) near the frequency of this mode. We calculate the interaction pattern that would be generated by doing so. This has the desired oscillatory pattern of ferromagnetic and antiferromagnetic interactions. Also the interaction strength decreases with distance as can be seen in figure 3.2. However a power-law regression analysis shows that it is not of the form of a power law. However the obtained interaction pattern has a ground state which can satisfy all the interactions. To observe frustration one must study

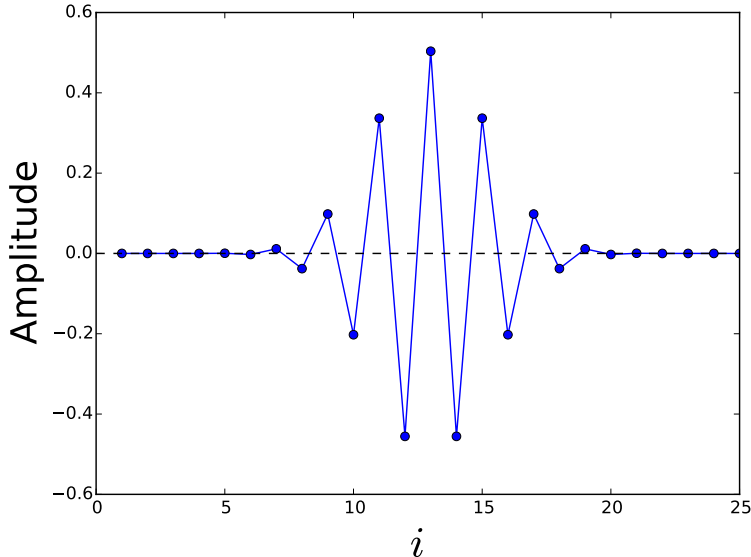


Figure 3.1: The lowest frequency transverse mode of a one-dimensional linear chain with 25 ions.

a two-dimensional system.

In section 2.2.1 we had seen that a triangular lattice is formed for 7, 19, 37... number of ions. We observe that in the lowest frequency transverse mode of such crystals all ions within a shell oscillate in-phase while ions in neighbouring shells oscillate out of phase (figure 3.3). This is analogous to the desired interaction pattern with respect to the central ion. Figure 3.4 shows the interaction pattern with respect to the central ion when one tunes the laser close to the frequency of this mode. For reference an RKKY interaction curve is also plotted. The wavelength of ferromagnetic-antiferromagnetic oscillation of the RKKY pattern thus generated is fixed and cannot be controlled by adjusting any parameters as it is a function of the phonon mode used. However the peripheral ions do not show such a pattern. Our analysis shows that in the 19 ions system 30 of the 130 two-spin interactions are along the wrong direction in the ground state of the system. This frustration however doesn't lead to degeneracy as the conflicting interactions are of weaker strength as compared to other interactions present in the system.

In many crystals with different number of ions than ones required to form triangular lattices it is observed that this oscillatory mode is not the lowest frequency transverse mode. However such a mode exists in such crystals also, just that it is within the band of transverse modes. It is hard to use a

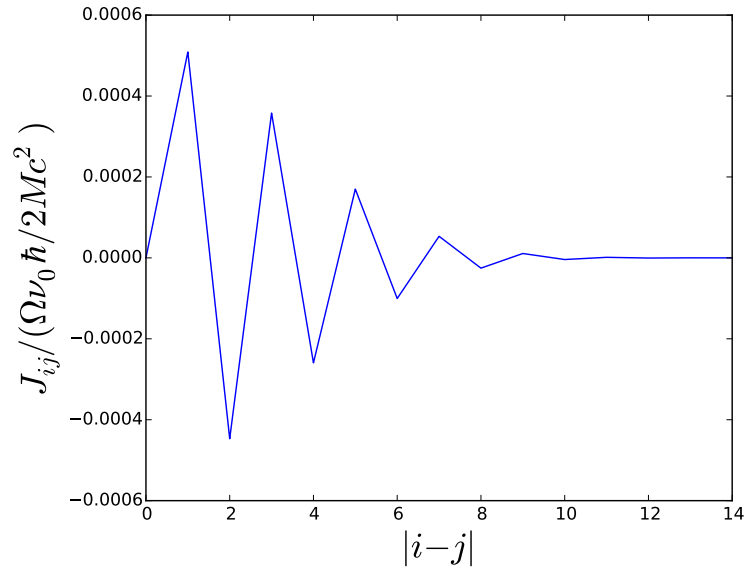


Figure 3.2: Resultant interaction pattern of the one-dimensional RKKY simulation. The graph has been calculated for a 25 ion chain with $\nu_x = \nu_y = 10$ and $\nu_z = 1$ and a detuning of $\delta = -0.1\nu_0$. This both the oscillatory as well as the diminishing nature of the RKKY interaction.

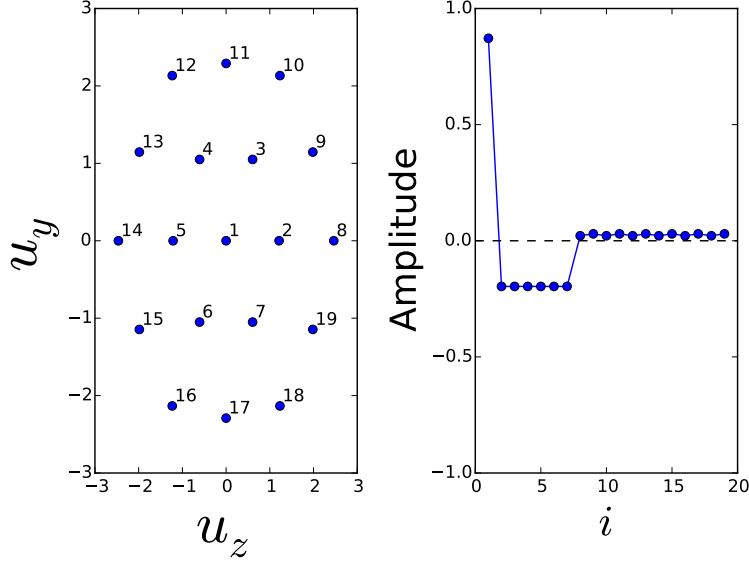


Figure 3.3: The plot on the left shows the positions of ions in a 19 ion chain, the indices of each ion has been marked near it. The plot on the right shows the lowest frequency transverse mode in this crystal, the relative amplitudes have been plotted against the index of the ion. This mode shall be used to simulate RKKY interactions. This has been calculated for 19 ions in a symmetric two dimensional trap with $\nu_z = \nu_y = 1$ and $\nu_x = 6$ and a detuning of $\delta = -0.1\nu_0$

mode which is inside a band since one is forced to use smaller and smaller detunings, which might lead to resonance effects. This is especially true when the number of ions is large as the band gets denser. Our analysis also shows that this mode has the largest amplitude for the central ion, in fact this mode has the largest amplitude for the central ion among all the transverse modes. Hence any changes to the central ion it will affect this mode the most. We can specifically change the trapping around a specific ion as demonstrated in [22]. Loosening the trapping near the central ion brings down the frequency of this mode thus taking it outside the band. This also helps with the triangular lattices, since even in this case this mode is removed from the rest of the band.

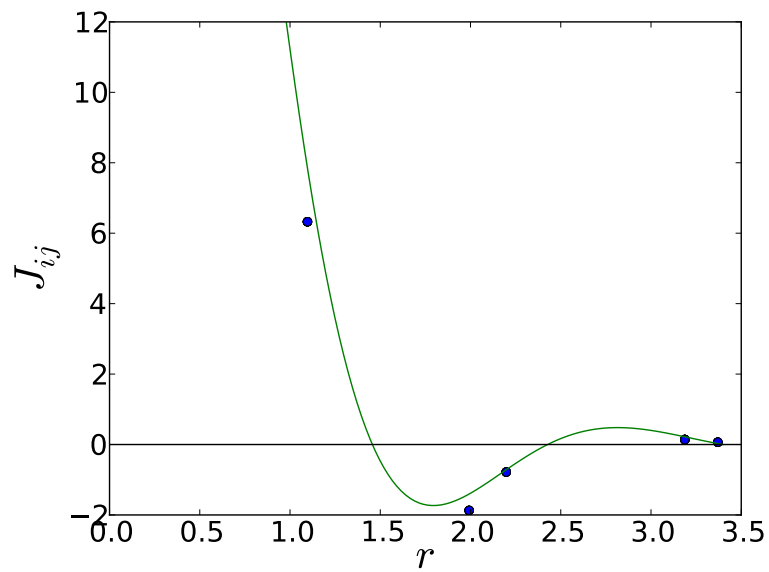


Figure 3.4: Here we plot the interaction strength J_{ij} as a function of the distance between them r . For reference $\cos(r)/r^3$ is also plotted. This shows the oscillating as well as the diminishing nature of the interaction. This has been calculated for 37 ions in a symmetric two dimensional trap with $\nu_z = \nu_y = 1$ and $\nu_x = 6$ and a detuning of $\delta = -0.1\nu_0$

3.2 Spin Glass with trapped ions

Using the method developed in simulating RKKY interactions, one can extend to simulation of spin glasses. We shall present to you preliminary work done in this direction and challenges that we face while developing such a system.

[57] study spin systems with randomly arranged spins under RKKY interactions using Monte-Carlo simulation. They were able to observe several properties also observed in spin glasses. In a similar vein we hope to simulate spin glasses using quantum systems. Already [58] have proposed a quantum system for spin glasses using quantum solids with impurities.

Firstly we look at how good is the naive RKKY model as a system to simulate spin glasses. We observe that there are no multiple energy wells in the potential energy spectrum of such a system. It is speculated that this is due to the small size of the system. In [57] multiple energy minima were observed only as the size of the system started approaching ≈ 150 . The essential ingredients for RKKY based spin glass is the irregularity in the interactions generated by a randomness of position and the frequent spin-flips of an RKKY interactions. In the system that we have been using such irregularity may not arise since the positions of all the ions are very regular.

One of the possible ways to solve this problem is to make the interaction pattern anisotropic. This would make the various spins at the same distance from a given spin not have similar interactions and thus would break the regularity of the interactions. Such anisotropic interactions have already been demonstrated in quantum simulations using trapped ions[25]. In their experiments the laser field used is not entirely perpendicular to the crystal plane, but at an angle. Although this might excite the longitudinal modes as well, if the laser frequency used is sufficiently far from those of the modes the interaction pattern will be unaffected. Upon using such techniques the sign of the interaction becomes rather irregular. We also calculate the probability distribution for a given interaction strength, It follows a centralized distribution which is akin to the Gaussian distribution of the Edwards et Anderson model.

There are still many challenges that have to be overcome such as 1) The ability to simulate temperature in the system 2) make the wavelength of oscillation of the sign of the interaction pattern controllable 3) Application of the method to larger systems and making sure that it stays scalable.

Chapter 4

Conclusion

In this thesis we first reviewed existing methods of quantum simulation of spin systems using trapped ions. We also showed how to create a two-dimensional crystal as well as an example of a quantum simulation. We have demonstrated how to create an RKKY interaction pattern in quantum spins in a triangular lattice. This work can be built upon to create a quantum simulation of spin glasses and our preliminary research is mildly promising with certain challenges that still need to be overcome.

Bibliography

- [1] R. P. Feynman, Simulating physics with computers, *International Journal of Theoretical Physics* 21 (6-7) (1982) 467–488. doi:[10.1007/BF02650179](https://doi.org/10.1007/BF02650179).
- [2] D. Deutsch, Quantum computational networks, *Proceedings of the Royal Society of London A: Mathematical, Physical and Engineering Sciences* 425 (1868) (1989) 73–90. doi:[10.1098/rspa.1989.0099](https://doi.org/10.1098/rspa.1989.0099).
- [3] P. Shor, Algorithms for quantum computation: discrete logarithms and factoring, in: *Foundations of Computer Science, 1994 Proceedings., 35th Annual Symposium on, 1994*, pp. 124–134. doi:[10.1109/SFCS.1994.365700](https://doi.org/10.1109/SFCS.1994.365700).
- [4] J. I. Cirac, P. Zoller, Quantum computations with cold trapped ions, *Physical review letters* 74 (20) (1995) 4091.
- [5] C. Monroe, D. M. Meekhof, B. E. King, W. M. Itano, D. J. Wineland, Demonstration of a fundamental quantum logic gate, *Phys. Rev. Lett.* 75 (1995) 4714–4717. doi:[10.1103/PhysRevLett.75.4714](https://doi.org/10.1103/PhysRevLett.75.4714).
- [6] S. Gulde, H. Häffner, M. Riebe, G. Lancaster, C. Becher, J. Eschner, F. Schmidt-Kaler, I. L. Chuang, R. Blatt, Quantum information processing with trapped ca+ ions, *Philosophical Transactions of the Royal Society of London A: Mathematical, Physical and Engineering Sciences* 361 (1808) (2003) 1363–1374. doi:[10.1098/rsta.2003.1206](https://doi.org/10.1098/rsta.2003.1206).
- [7] M. Barret, J. Chiaverini, T. Schaetz, J. Britton, W. Itano, J. Jost, E. Knill, C. Langer, D. Leibfried, R. Ozeri, D. Wineland, Deterministic quantum teleportation of atomic qubits, *Nature* 429 (2004) 737–739. doi:[10.1038/nature02570](https://doi.org/10.1038/nature02570).
- [8] M. Riebe, H. Häffner, C. Roos, W. Hänsel, J. Benhelm, G. Lancaster, T. Körber, C. Becher, F. Schmidt-Kaler, D. James, et al., Deterministic

- quantum teleportation with atoms, *Nature* 429 (6993) (2004) 734–737. doi:[10.1038/nature02570](https://doi.org/10.1038/nature02570).
- [9] J. Chiaverini, D. Leibfried, T. Schaetz, M. Barrett, R. Blakestad, J. Britton, W. Itano, J. Jost, E. Knill, C. Langer, et al., Realization of quantum error correction, *Nature* 432 (7017) (2004) 602–605. doi:[10.1038/nature03074](https://doi.org/10.1038/nature03074).
- [10] R. Schmied, J. H. Wesenberg, D. Leibfried, Quantum simulation of the hexagonal kitaev model with trapped ions, *New Journal of Physics* 13 (11) (2011) 115011. URL <http://stacks.iop.org/1367-2630/13/i=11/a=115011>
- [11] J. Casanova, A. Mezzacapo, L. Lamata, E. Solano, Quantum simulation of interacting fermion lattice models in trapped ions, *Phys. Rev. Lett.* 108 (2012) 190502. doi:[10.1103/PhysRevLett.108.190502](https://doi.org/10.1103/PhysRevLett.108.190502). URL <http://link.aps.org/doi/10.1103/PhysRevLett.108.190502>
- [12] A. Friedenauer, H. Schmitz, J. T. Glueckert, D. Porras, T. Schaetz, Simulating a quantum magnet with trapped ions, *Nature Physics* 4 (2008) 757–761. doi:[10.1038/nphys1032](https://doi.org/10.1038/nphys1032).
- [13] K. Kim, M.-S. Chang, R. Islam, S. Korenblit, L.-M. Duan, C. Monroe, Entanglement and tunable spin-spin couplings between trapped ions using multiple transverse modes, *Phys. Rev. Lett.* 103 (2009) 120502. doi:[10.1103/PhysRevLett.103.120502](https://doi.org/10.1103/PhysRevLett.103.120502). URL <http://link.aps.org/doi/10.1103/PhysRevLett.103.120502>
- [14] E. E. Edwards, S. Korenblit, K. Kim, R. Islam, M.-S. Chang, J. K. Freericks, G.-D. Lin, L.-M. Duan, C. Monroe, Quantum simulation and phase diagram of the transverse-field ising model with three atomic spins, *Phys. Rev. B* 82 (2010) 060412. doi:[10.1103/PhysRevB.82.060412](https://doi.org/10.1103/PhysRevB.82.060412). URL <http://link.aps.org/doi/10.1103/PhysRevB.82.060412>
- [15] B. P. Lanyon, C. Hempel, D. Nigg, M. M̄ajller, R. Gerritsma, F. ZÄdhringer, P. Schindler, J. T. Barreiro, M. Rambach, G. Kirchmair, M. Hennrich, P. Zoller, R. Blatt, C. F. Roos, Universal digital quantum simulation with trapped ions, *Science* 334 (6052) (2011) 57–61. arXiv: <http://www.sciencemag.org/content/334/6052/57.full.pdf>, doi: [10.1126/science.1208001](https://doi.org/10.1126/science.1208001). URL <http://www.sciencemag.org/content/334/6052/57.abstract>
- [16] J. W. Britton, B. C. Sawyer, A. C. Keith, C.-C. J. Wang, J. K. Freericks, H. Uys, M. J. Biercuk, J. J. Bollinger, Engineered two-dimensional ising

- interactions in a trapped-ion quantum simulator with hundreds of spins, *Nature* 484 (7395) (2012) 489–492. doi:[10.1038/nature10981](https://doi.org/10.1038/nature10981).
- [17] K. Kim, M.-S. Chang, S. Korenblit, R. Islam, E. Edwards, J. Freericks, G.-D. Lin, L.-M. Duan, C. Monroe, Quantum simulation of frustrated ising spins with trapped ions, *Nature* 465 (7298) (2010) 590–593. doi:[10.1038/nature09071](https://doi.org/10.1038/nature09071).
- [18] R. Islam, C. Senko, W. C. Campbell, S. Korenblit, J. Smith, A. Lee, E. E. Edwards, C.-C. J. Wang, J. K. Freericks, C. Monroe, [Emergence and frustration of magnetism with variable-range interactions in a quantum simulator](#), *Science* 340 (6132) (2013) 583–587. arXiv:<http://www.sciencemag.org/content/340/6132/583.full.pdf>, doi:[10.1126/science.1232296](https://doi.org/10.1126/science.1232296).
URL <http://www.sciencemag.org/content/340/6132/583.abstract>
- [19] A. Bermudez, J. Almeida, K. Ott, H. Kaufmann, S. Ulm, U. Poschinger, F. Schmidt-Kaler, A. Retzker, M. B. Plenio, [Quantum magnetism of spin-ladder compounds with trapped-ion crystals](#), *New Journal of Physics* 14 (9) (2012) 093042.
URL <http://stacks.iop.org/1367-2630/14/i=9/a=093042>
- [20] P. Richerme, Z.-X. Gong, A. Lee, C. Senko, J. Smith, M. Foss-Feig, S. Michalakis, A. V. Gorshkov, C. Monroe, Non-local propagation of correlations in quantum systems with long-range interactions, *Nature* 511 (7508) (2014) 198–201. doi:[10.1038/nature13450](https://doi.org/10.1038/nature13450).
- [21] P. Jurcevic, B. P. Lanyon, P. Hauke, C. Hempel, P. Zoller, R. Blatt, C. F. Roos, Quasiparticle engineering and entanglement propagation in a quantum many-body system, *Nature* 511 (7508) (2014) 202–205. doi:[10.1038/nature13461](https://doi.org/10.1038/nature13461).
- [22] j. v. n. p. u. y. Nath, R. and Dalmonte, M. and Glaetzle, A. W. and Zoller, P. and Schmidt-Kaler, F. and Gerritsma R., title=Hexagonal plaquette spin–spin interactions and quantum magnetism in a two-dimensional ion crystal.
- [23] D. Porras, J. I. Cirac, [Effective quantum spin systems with trapped ions](#), *Phys. Rev. Lett.* 92 (2004) 207901. doi:[10.1103/PhysRevLett.92.207901](https://doi.org/10.1103/PhysRevLett.92.207901).
URL <http://link.aps.org/doi/10.1103/PhysRevLett.92.207901>

- [24] D. Porras, J. I. Cirac, [Quantum manipulation of trapped ions in two dimensional coulomb crystals](#), *Phys. Rev. Lett.* 96 (2006) 250501. doi:
[10.1103/PhysRevLett.96.250501](https://doi.org/10.1103/PhysRevLett.96.250501).
URL <http://link.aps.org/doi/10.1103/PhysRevLett.96.250501>
- [25] A. Bermudez, J. Almeida, F. Schmidt-Kaler, A. Retzker, M. Plenio, [Frustrated quantum spin models with cold coulomb crystals](#), *Phys. Rev. Lett.* 107 (207209). doi:
[10.1103/PhysRevLett.107.207209](https://doi.org/10.1103/PhysRevLett.107.207209).
- [26] D. J. Wineland, C. Monroe, W. M. Itano, L. D., K. B. E., M. D. M., [Experimental issues in coherent quantum-state manipulation of trapped atomic ions](#), *Journal of Research of National Institute of Standards and Technology* 103 (3) (1998) 259–328. doi:
[10.6028/jres.103.019](https://doi.org/10.6028/jres.103.019).
- [27] M. Šašura, V. Bužek, [Cold trapped ions as quantum information processors](#), *Journal of Modern Optics* 49 (10) (2002) 1593–1647. doi:
[10.1080/09500340110115497](https://doi.org/10.1080/09500340110115497).
- [28] H. Häffner, C. Roos, R. Blatt, [Quantum computing with trapped ions](#), *Physics Reports* 469 (4) (2008) 155–203. doi:
[10.1016/j.physrep.2008.09.003](https://doi.org/10.1016/j.physrep.2008.09.003).
URL <http://www.sciencedirect.com/science/article/pii/S0370157308003463>
- [29] D. Leibfried, R. Blatt, C. Monroe, D. Wineland, [Quantum dynamics of single trapped ions](#), *Rev. Mod. Phys.* 75 (2003) 281–324. doi:
[10.1103/RevModPhys.75.281](https://doi.org/10.1103/RevModPhys.75.281).
URL <http://link.aps.org/doi/10.1103/RevModPhys.75.281>
- [30] R. Blatt, D. Wineland, [Entangled states of trapped atomic ions](#), *Nature* 453 (7198) (2008) 1008–1015. doi:
[10.1038/nature07125](https://doi.org/10.1038/nature07125).
- [31] R. Blatt, C. F. Roos, [Quantum simulations with trapped ions](#), *Nature Physics* 8 (2012) 277–284. doi:
[10.1038/nphys2252](https://doi.org/10.1038/nphys2252).
- [32] C. Schneider, D. Porras, T. Schaetz, [Experimental quantum simulations of many-body physics with trapped ions](#), *Reports on Progress in Physics* 75 (2) (2012) 024401. doi:
[10.1088/0034-4885/75/2/024401](https://doi.org/10.1088/0034-4885/75/2/024401).
URL <http://stacks.iop.org/0034-4885/75/i=2/a=024401>
- [33] C. Kittel, [Indirect exchange interactions in metals*](#), Vol. 22 of *Solid State Physics*, Academic Press, 1969, pp. 1 – 26. doi:
[http://dx.doi.org/10.1016/S0081-1947\(08\)60030-2](http://dx.doi.org/10.1016/S0081-1947(08)60030-2).

URL <http://www.sciencedirect.com/science/article/pii/S0081194708600302>

- [34] M. A. Ruderman, C. Kittel, Indirect exchange coupling of nuclear magnetic moments by conduction electrons, *Phys. Rev.* 96 (1954) 99–102. doi:10.1103/PhysRev.96.99.
URL <http://link.aps.org/doi/10.1103/PhysRev.96.99>
- [35] T. Kasuya, A theory of metallic ferro- and antiferromagnetism on zener's model, *Progress of Theoretical Physics* 16 (1) (1956) 45–57. arXiv:<http://ptp.oxfordjournals.org/content/16/1/45.full.pdf+html>, doi:10.1143/PTP.16.45.
URL <http://ptp.oxfordjournals.org/content/16/1/45.abstract>
- [36] K. Yosida, Magnetic properties of cu-mn alloys, *Phys. Rev.* 106 (1957) 893–898. doi:10.1103/PhysRev.106.893.
URL <http://link.aps.org/doi/10.1103/PhysRev.106.893>
- [37] P. Phillips, *Advanced Solid State Physics*, Cambridge University Press, 2002.
- [38] K. Binder, A. P. Young, Spin glasses: Experimental facts, theoretical concepts, and open questions, *Rev. Mod. Phys.* 58 (1986) 801–976. doi:10.1103/RevModPhys.58.801.
URL <http://link.aps.org/doi/10.1103/RevModPhys.58.801>
- [39] S. Edwards, P. Anderson, Theory of spin glasses, *J. Phys. F* 5 (1975) 965–974.
- [40] D. L. Stein, C. M. Newman, *Spin Glasses and complexity*, Princeton University Press, 2013.
- [41] H. Landa, M. Drewsen, B. Reznik, A. Retzker, Modes of oscillation in radiofrequency paul traps, *New Journal of Physics* 14 (9) (2012) 093023. URL <http://stacks.iop.org/1367-2630/14/i=9/a=093023>
- [42] H. Landa, M. Drewsen, B. Reznik, A. Retzker, Classical and quantum modes of coupled mathieu equations, *Journal of Physics A: Mathematical and Theoretical* 45 (45) (2012) 455305.
URL <http://stacks.iop.org/1751-8121/45/i=45/a=455305>
- [43] H. Kaufmann, S. Ulm, G. Jacob, U. Poschinger, H. Landa, A. Retzker, M. B. Plenio, F. Schmidt-Kaler, Precise experimental investigation of eigenmodes in a planar ion crystal, *Phys. Rev. Lett.* 109 (2012) 263003.

doi:10.1103/PhysRevLett.109.263003.

URL <http://link.aps.org/doi/10.1103/PhysRevLett.109.263003>

- [44] B. Yoshimura, M. Stork, D. Dacic, W. C. Campbell, J. K. Freericks, Creation of two-dimensional coulomb crystals of ions in oblate paul traps for quantum simulations. [arXiv:1406.5545](https://arxiv.org/abs/1406.5545).
- [45] W. M. Itano, J. J. Bollinger, J. N. Tan, B. Jelenković, X.-P. Huang, D. J. Wineland, Bragg diffraction from crystallized ion plasmas, *Science* 279 (5351) (1998) 686–689. [arXiv:http://www.sciencemag.org/content/279/5351/686.full.pdf](https://arxiv.org/abs/http://www.sciencemag.org/content/279/5351/686.full.pdf), doi:10.1126/science.279.5351.686.
URL <http://www.sciencemag.org/content/279/5351/686.abstract>
- [46] T. B. Mitchell, J. J. Bollinger, D. H. E. Dubin, X.-P. Huang, W. M. Itano, R. H. Baughman, Direct observations of structural phase transitions in planar crystallized ion plasmas, *Science* 282 (5392) (1998) 1290–1293. [arXiv:http://www.sciencemag.org/content/282/5392/1290.full.pdf](https://arxiv.org/abs/http://www.sciencemag.org/content/282/5392/1290.full.pdf), doi:10.1126/science.282.5392.1290.
URL <http://www.sciencemag.org/content/282/5392/1290.abstract>
- [47] J. I. Cirac, P. Zoller, A scalable quantum computer with ions in an array of microtraps, *Nature* 404 (6778) (2000) 579–581. doi:10.1038/35007021.
- [48] D. Kielpinski, C. Monroe, D. J. Wineland, Architecture for a large-scale ion-trap quantum computer, *Nature* 417 (6890) (2002) 709–711. doi:10.1038/nature00784.
- [49] C. Monroe, J. Kim, Scaling the ion trap quantum processor, *Science* 339 (6124) (2013) 1164–1169. [arXiv:http://www.sciencemag.org/content/339/6124/1164.full.pdf](https://arxiv.org/abs/http://www.sciencemag.org/content/339/6124/1164.full.pdf), doi:10.1126/science.1231298.
URL <http://www.sciencemag.org/content/339/6124/1164.abstract>
- [50] D. James, Quantum dynamics of cold trapped ions with application to quantum computation, *Appl. Phys. B* 66 (2) (1998) 181–190.
- [51] D. Knoll, D. Keyes, Jacobian-free newton-krylov methods: a survey of approaches and applications, *J. Comp. Phys.* 193 (2) (2004) 357–397. doi:http://dx.doi.org/10.1016/j.jcp.2003.08.010.

URL <http://www.sciencedirect.com/science/article/pii/S0021999103004340>

- [52] E. Jones, T. Oliphant, P. Peterson, et al., *SciPy: Open source scientific tools for Python*, [Online; accessed 2015-03-24] (2001–).
URL <http://www.scipy.org/>
- [53] E. Anderson, Z. Bai, C. Bischof, S. Blackford, J. Demmel, J. Dongarra, J. Du Croz, A. Greenbaum, S. Hammarling, A. McKenney, D. Sorensen, *LAPACK Users' Guide*, 3rd Edition, Society for Industrial and Applied Mathematics, Philadelphia, PA, 1999.
- [54] R. B. Lehoucq, D. C. Sorensen, C. Yang, *Arpack users guide: Solution of large scale eigenvalue problems by implicitly restarted arnoldi methods*. (1997).
- [55] J. D. Hunter, *Matplotlib: A 2d graphics environment*, *Computing In Science & Engineering* 9 (3) (2007) 90–95.
- [56] T. Grasz, M. Lewenstein, *Trapped-ion quantum simulation of tunable range heisenberg chains*, *EPJ Quantum Technology* 1 (1) (2014) 8. doi: [1140/epjqt8](https://doi.org/10.1140/epjqt8).
- [57] L. Walker, R. Walstedt, *Computer studies of rkky spin glasses*, *Journal of Magnetism and Magnetic Materials* 31–34, Part 3 (1983) 1289 – 1292. doi: [10.1016/0304-8853\(83\)90899-5](https://doi.org/10.1016/0304-8853(83)90899-5).
- [58] M. Lemeshko, N. Y. Yao, A. V. Gorshkov, H. Weimer, S. D. Bennet, T. Momose, G. Sarang, *Controllable quantum spin glasses with magnetic impurities embedded in quantum solids*, *Phys. Rev. B* 88 (14426).

Appendix A

Long proofs

All supplementary material that adds to the body of work of the main text should be added here. The use of supplementary information in the form of Appendices is non-mandatory. Please use them only if you feel that they are essential in clarifying parts of the main text of the project report. If you find it necessary, you can add more than one of them. (Appendix 2, 3 etc)

A.1 Determining the equilibrium configuration of two dimensional crystals

The potential experienced by ions is given in equation (2.3) reproduced below:

$$V = \frac{1}{2}M\nu_0^2l^2 \left(\sum_{\substack{i,d=1,1 \\ i \neq j}}^{N,3} \nu_d^2 u_{d,i}^2 + \sum_{\substack{i,j=1,1 \\ i \neq j}}^{N,N} \frac{1}{u_{ij}} \right) \quad (\text{A.1})$$

An equilibrium configuration of positions of ions would correspond to a minimum in the above function. At a minimum all the derivatives of the potential energy function would vanish i.e. $\partial V/\partial x_{d_i,i} = 0 \forall 1 \leq d_i \leq 3, 1 \leq i \leq N$.

$$\frac{\partial V}{\partial x_{d_i,i}} = \frac{\partial V}{\partial u_{d_i,i}} \frac{\partial u_{d_i,i}}{\partial x_{d_i,i}} \text{ and, } \frac{\partial u_{d_i,i}}{\partial x_{d_i,i}} = l^{-1} \quad (\text{A.2})$$

hence,

$$\begin{aligned}
\frac{\partial V}{\partial x_{d_i,i}} &= \frac{1}{2} M \nu_0^2 l \frac{\partial}{\partial u_{d_i,i}} \left(\sum_{j,d=1,1}^{N,3} \nu_d^2 u_{d,j}^2 + \sum_{\substack{j,k=1,1 \\ j \neq k}}^{N,N} \left(\sum_{d=1}^3 (u_{d,j} - u_{d,k})^2 \right)^{-1/2} \right) \\
&= M \nu_0^2 l \left(\nu_{d_i}^2 u_{d_i,i} - \sum_{\substack{j=1 \\ j \neq i}}^N (u_{d_i,i} - u_{d_i,j}) \left(\sum_{d=1}^3 (u_{d,j} - u_{d,k})^2 \right)^{-3/2} \right)
\end{aligned} \tag{A.3}$$

which can be rewritten as equation (2.4).

Calculation of the phonon modes requires the calculation of the second derivative of the potential energy function. i.e. $\frac{\partial^2 V}{\partial x_{d_i,i} \partial x_{d_j,j}}$.

$$\frac{\partial^2 V}{\partial x_{d_i,i} \partial x_{d_j,j}} = M \nu_0^2 \frac{\partial}{\partial x_{d_j,j}} \left(\nu_{d_i}^2 u_{d_i,i} - \sum_{\substack{k=1 \\ k \neq i}}^N \frac{(u_{d_i,i} - u_{d_i,k})}{\left(\sum_{d=1}^3 (u_{d,i} - u_{d,k})^2 \right)^{3/2}} \right) \tag{A.4}$$

This can be further divided into four cases:

Case I: $i = j$ and $d_i = d_j$

$$\frac{\partial^2 V}{\partial x_{d_i,i} \partial x_{d_i,i}} = M \nu_0^2 \left(\nu_{d_i}^2 - \sum_{\substack{k=1 \\ k \neq i}}^N \left(\frac{1}{u_{ik}^3} - \frac{3(u_{d_i,i} - u_{d_i,k})^2}{u_{ik}^5} \right) \right) \tag{A.5}$$

Case II: $i \neq j$ and $d_i = d_j$

$$\frac{\partial^2 V}{\partial x_{d_i,i} \partial x_{d_i,j}} = M \nu_0^2 \left(\frac{1}{u_{ij}^3} - \frac{3(u_{d_i,i} - u_{d_i,j})^2}{u_{ij}^5} \right) \tag{A.6}$$

Case III: $i = j$ and $d_i \neq d_j$

$$\frac{\partial^2 V}{\partial x_{d_i,i} \partial x_{d_j,i}} = \sum_{\substack{k=1 \\ k \neq i}}^N \frac{3(u_{d_i,i} - u_{d_i,k})(u_{d_j,i} - u_{d_j,k})}{u_{ik}^5} \tag{A.7}$$

Case IV: $i \neq j$ and $d_i \neq d_j$

$$\frac{\partial^2 V}{\partial x_{d_i,i} \partial x_{d_j,j}} = - \frac{3(u_{d_i,i} - u_{d_i,j})(u_{d_j,i} - u_{d_j,j})}{u_{ij}^5} \tag{A.8}$$

Adding these cases we can arrive at equation (2.5).

A.2 Derivation of the spin-spin Hamiltonian

We can write \vec{x} as a sum of position operators of all phonon modes. Hence

$$\vec{x}_i = \sum_{m=1}^{3N} \vec{b}_{mi} \sqrt{\frac{\hbar}{2M\omega_m}} (\hat{a}_m^\dagger + \hat{a}_m) \quad (\text{A.9})$$

We shall introduce Lamb-Dicke parameters as

$$\vec{k} \cdot \vec{x}_i = \sum_{m=1}^{3N} \eta_{mi} (\hat{a}_m^\dagger + \hat{a}_m) \quad (\text{A.10})$$

They represent the strength of the coupling created between the electronic states and the motional states by the optical field. They can be defined using

$$\eta_{mi} = \vec{k} \cdot \vec{b}_{mi} \sqrt{\frac{\hbar}{2M\omega_m}} \quad (\text{A.11})$$

Incorporating equations (A.9) and (A.10) into (2.8) we get

$$\hat{H}_I = \sum_{i=1}^N \hbar\Omega \left(e^{i(\sum_{m=1}^{3N} \eta_{mi} (\hat{a}_m^\dagger + \hat{a}_m) + \omega_I t + \phi_i)} + \text{h.c.} \right) \hat{\kappa}_i \quad (\text{A.12})$$

The total Hamiltonian of the system becomes

$$\hat{H} = \underbrace{\hat{H}_e + \hat{H}_m}_{\hat{H}_0} + \hat{H}_I \quad (\text{A.13})$$

We shall write the Hamiltonian in the interaction picture using \hat{H}_0 as the known part of the Hamiltonian. In the interaction picture the interaction Hamiltonian will be

$$\hat{H}'_I(t) = \hat{U}_0^\dagger(t) \hat{H}_I \hat{U}_0(t) \text{ where } \hat{U}_0(t) = e^{-i\hat{H}_0 t/\hbar} \quad (\text{A.14})$$

Since both $\hat{U}_0(t)$ and \hat{H}_I are separable with respect to individual ions, the transformation into to interaction picture can be done separately for each ion.

$$\hat{H}'_I(t) = \sum_{i=1}^N \hat{H}'_{Ii} \quad (\text{A.15})$$

Also since the electronic part and motional part are independent this can be broken down into:

$$\hat{\mathcal{H}}_I i' = \underbrace{e^{i\hat{\mathcal{H}}_m t/\hbar} \hbar\Omega \left(e^{i(\sum_{m=1}^{3N} \eta_i^m (\hat{a}_m^\dagger + \hat{a}_m) + \omega_I t + \phi_i)} + \text{h.c.} \right)}_{\text{Part 1}} \underbrace{e^{-i\hat{\mathcal{H}}_m t/\hbar} e^{i\hat{\mathcal{H}}_e t/\hbar} \hat{\kappa}_i e^{-i\hat{\mathcal{H}}_e t/\hbar}}_{\text{Part 2}} \quad (\text{A.16})$$

Part 2 can be simplified as:

$$\begin{aligned} \hat{\kappa}_i' &= e^{i\hat{\mathcal{H}}_e t/\hbar} \hat{\kappa}_i e^{-i\hat{\mathcal{H}}_e t/\hbar} \\ &= e^{i\omega t \hat{\sigma}_i^z/2} (\alpha_0 \hat{\mathbb{1}}_i + \alpha_1 \hat{\sigma}_i^x + \alpha_2 \hat{\sigma}_i^y + \alpha_3 \hat{\sigma}_i^z) e^{-i\omega t \hat{\sigma}_i^z/2} \\ &= e^{i\omega t \hat{\sigma}_i^z/2} (\alpha_0 \hat{\mathbb{1}}_i + \alpha_3 \hat{\sigma}_i^z + 1/2(\alpha_1 - i\alpha_2) \hat{\sigma}_i^+ + 1/2(\alpha_1 + i\alpha_2) \hat{\sigma}_i^-) e^{-i\omega t \hat{\sigma}_i^z/2} \\ &= \frac{1}{2} (\alpha_0 \hat{\mathbb{1}}_i + (\alpha_1 - i\alpha_2) e^{i\omega t} \hat{\sigma}_i^+ + \alpha_3 \hat{\sigma}_i^z) + \text{h.c.} \end{aligned}$$

Part 1 contains terms of the form

$$e^{i\omega_I t \hat{a}_m^\dagger \hat{a}_m} e^{i\eta_i^m (\hat{a}_m^\dagger + \hat{a}_m)} e^{-i\omega_I t \hat{a}_m^\dagger \hat{a}_m} \quad (\text{A.17})$$

Using the Baker-Campbell-Hausdorff formula

$$e^{-\hat{B}} \hat{A} e^{-\hat{B}} = \sum_n \frac{1}{n!} [\hat{A}, \hat{B}]^{\{n\}} \quad (\text{A.18})$$

and the commutation relation for harmonic oscillator annihilation operator

$$[\hat{a}, \hat{a}^\dagger] = \mathbb{1} \quad (\text{A.19})$$

one can get

$$e^{i\eta_i^m} \exp(\hat{a}_m e^{-i\omega_I t} + \hat{a}_m^\dagger e^{i\omega_I t}) = e^{i\omega_I t \hat{a}_m^\dagger \hat{a}_m} e^{i\eta_i^m (\hat{a}_m^\dagger + \hat{a}_m)} e^{-i\omega_I t \hat{a}_m^\dagger \hat{a}_m} \quad (\text{A.20})$$

which gives us the interaction Hamiltonian

$$\hat{\mathcal{H}}_{Ii} = \left(\hbar\Omega \exp \left(\sum_{m=1}^{3N} i\eta_i^m (\hat{a}_m e^{-i\omega_I t} + \hat{a}_m^\dagger e^{i\omega_I t}) - i\omega_I t + i\phi_i \right) + \text{h.c.} \right) \hat{\kappa}_i' \quad (\text{A.21})$$

We shall assume $\omega_I \ll \omega$. We will apply the rotating wave approximation in which terms which rotate too fast are averaged out. In this case we neglect terms not having $e^{i\omega_I t}$ to get

$$\hat{\mathcal{H}}_I^{(i)} = \hbar\Omega \exp \left(\sum_{m=1}^{3N} i\eta_i^m (\hat{a}_m e^{-i\omega_I t} + \hat{a}_m^\dagger e^{i\omega_I t}) - i\omega_I t + i\phi_i \right) (\alpha_0 \hat{\mathbb{1}}_i + \alpha_3 \hat{\sigma}_i^z) + \text{h.c.} \quad (\text{A.22})$$

We use the Hamiltonian (A.22) to create an effective $\hat{\sigma}^z \otimes \hat{\sigma}^z$ interaction and hence an Ising like Hamiltonian. We shall assume that we are working in the Lamb-Dicke regime, where the induced coupling between the motional states and the electronic states are small. Here $\eta \langle (\hat{a}_m^\dagger + \hat{a}_m)^2 | (\hat{a}_m^\dagger + \hat{a}_m)^2 \rangle^{1/2} \ll 1$. Hence expanding the Hamiltonian in terms of the Lamb-Dicke parameters and ignoring all higher order terms other than the linear term.

$$\hat{\mathcal{H}}'_I = \hbar\Omega e^{-i\omega_I t + i\phi_i} \left(i \sum_{m=1}^{3N} \eta_i^m (\hat{a}_m e^{-i\omega_I t} + \hat{a}_m^\dagger e^{i\omega_I t}) \right) (\alpha_0 \hat{\mathbb{1}}_i + \alpha_3 \hat{\sigma}_i^z) + \text{h.c.} \quad (\text{A.23})$$

Using the Rotating wave approximation again and ignoring terms faster than $e^{i\delta t}$ we get:

$$\hat{\mathcal{H}}'_I = i\hbar\Omega \sum_{m=1}^{3N} \eta_i^m e^{i\phi_i} \hat{a}_m^\dagger (\alpha_0 \hat{\mathbb{1}}_i + \alpha_3 \hat{\sigma}_i^z) + \text{h.c.} \quad (\text{A.24})$$

The complete interaction Hamiltonian will also have the term $\hat{\mathcal{H}}_\delta$ which we had left out so far. However this part is unaffected by the transformation and can be written as it is in the final Hamiltonian. Hence

$$\hat{\mathcal{H}}'_S = \hat{\mathcal{H}}'_I + \hat{\mathcal{H}}_\delta \quad (\text{A.25})$$

Now we shall apply a canonical transformation to the above Hamiltonian such that its form becomes similar to that of the Ising Hamiltonian. The applied transformation is given by

$$\hat{\mathcal{H}}''_S = \hat{U} \hat{\mathcal{H}}'_S \hat{U}^\dagger \quad (\text{A.26})$$

with

$$\hat{U} = \exp \left(- \sum_{i=1}^N \sum_{m=1}^{3N} \frac{1}{\hbar\delta_m} \left(\hat{\xi}_i^m \hat{a}_m^\dagger - \hat{\xi}_i^{m\dagger} \hat{a}_m \right) \right) \quad (\text{A.27})$$

and

$$\hat{\xi}_i^m = i\hbar\Omega \eta_i^m e^{i\phi_i} (\alpha_0 \hat{\mathbb{1}}_i + \alpha_3 \hat{\sigma}_i^z) \quad (\text{A.28})$$

The transformed Hamiltonian is

$$\hat{\mathcal{H}}''_S = \sum_{i=1}^N \sum_{j=1}^N \sum_{m=1}^{3N} \frac{\Omega^2 \eta_i^m \eta_j^m}{\delta_m} e^{i\phi_i - \phi_j} (\alpha_0 \hat{\mathbb{1}}_i + \alpha_3 \hat{\sigma}_i^z) (\alpha_0 \hat{\mathbb{1}}_j + \alpha_3 \hat{\sigma}_j^z) + \hat{\mathcal{H}}_\delta \quad (\text{A.29})$$